A High-Speed Serial Digital Interface Video Signal Jitter Measurement Method

Difei Li, He Chen, Hongying Gao, Kejia Zhao, Zhaochun Wu and Bo Li

Electronics and Information Technology Division, National Institute of Metrology, China.No.18 Bei San Huan Dong Lu, Beijing, China

E-mail: {lidf & chenhe & gaohy & zhaokj & wuzc & libo}@nim.ac.cn

Abstract. This paper designs a measurement method for high-speed serial digital interface video signal jitter. Firstly, we introduce the features of SDI signal and the jitter measurement methods of traditional high-speed serial signals. A jitter model is built for the SDI signal while the properties of the components are analysed. An adjusted dual-Dirac model is adopted to measure the jitter in the signal. This method can accurately analyse different jitter components in SDI signals. It is directly performed on oscilloscope, which is beneficial to the traceability of the jitter. The feasibility of the method is verified by experiments. The measurement results show that the method has better measurement accuracy than the direct spectrum method.

1. Introduction

Serial digital interface (SDI) is a kind of digital video interfaces first standardized by SMPTE (The Society of Motion Picture and Television Engineers) in 1989 [1, 2]. SDI video signal transmission belongs to the mode of baseband serial signal communication. With the development of digital TV broadcasting network technology and related consumer electronics industry, digital video has already moved from full HD to 4K-HD or even 8K-HD. Utra-HD video will become the mainstream development direction of digital TV in the future that require greater fidelity and resolution than standard full HDTV can provide. 6G-SDI and 12G-SDI standards have been published which are prepared for transmission of uncompressed, high capacity and high bit rate digital video signals within video facilities [3, 4].

In the transmission of high-speed SDI signals, the performance of the whole system is often greatly affected due to the existence of jitter. Therefore, jitter has become a key factor restricting the design of high-speed digital systems [5]. As can be seen from the current various high-speed serial bus specifications, the jitter components of the SDI transmission system are extremely explicit. In order to ensure the stability of the high-speed digital system, it is necessary to accurately determine the jitter component of its existence and separate the different jitter components to determine whether the system performance meets the design requirements of bit error rate and stability while minimize the system due to jitter error.

At present, the measurement of serial signals mainly adopts an eye diagram analysis method that only used for qualitative measurement. An eye diagram is a graph of a series of digital signals accumulated on an oscilloscope. From the eye diagram, the effects of crosstalk and noise between codes can be observed which reflects the overall characteristics of the digital signal. That is, directly observing the shape of the eye to judge the quality of the signal. It is impossible to quantitatively measure the jitter component contained in the total jitter. From the eye diagram, we can only obtain the peak-to-peak value of jitters at the current moment [6].

Rising bit-rate result in smaller unit intervals and increasingly tighter timing budgets, thus, can even distinguish the difference in picosecond magnitude. In the past 10 years, the technology used to measure jitter in high-speed serial data signals has made great progress. The goal of all researches is to accurately measure the jitter value when the signal having the extremely low bit error rate (the BER) (e.g. 10^{-12}). Determining jitter at very small bit error ratios on a real-time oscilloscope requires algorithms that extrapolate the measured data rather than by simply calculating peak-to-peak or RMS values directly from the acquired measurements. An important reason for using extrapolation is that if the total jitter is measured directly, the measurement time required is very long and may even take a whole day. Therefore, extrapolation method was used.

The method of spectral measurement (jitter and signal quality specification methodology) which is used in the "MJSQ" in a dual-Dirac jitter model of a communication channel technology has become an industry standard [7]. This paper provides a complete method to measure jitters in high speed SDI video signal by using adjusted dual-Dirac model. This model illustrates the process of converting time interval error (TIE) measurements into jitter values and describes how to represent the view of the jitter components.

2. SDI signal jitter

As shown in Figure 1. In a digital communication link, jitter is the offset between the predicted position of the signal transition and the actual position of the transition. In serial data communication, jitter is a core issue to be aware of because excessive jitter in the transmitter data signal can cause data recovery errors at the receiver. To prevent the bit error rate from being too high, jitter margins are specified in many standards so that the transmit and receive circuits can be designed to operate within jitter budgets and tolerances. To ensure that the equipment works within these budgets, it is necessary to accurately measure jitter. Measurements not only quantify jitter, but also help designers examine the causes and sources of jitter to help reduce or eliminate value of jitter. The deviation faster than 10HZ is defined as jitter, and the deviation over 10Hz is defined as wander. Ideally, the time interval in SDI signals should as wide as the integer multiple of the unit interval (UI) [8]. UI is serial digital signal clock unit corresponds to the crystal oscillator frequency of SDI generator instrument. According to the SMPTE standard specification SDI signal bit rate amount to the clock frequency used to create SDI signal. During the actual transmission of the SDI signal, the transition position of the rising and falling edges of the signal will deviate from the ideal position [9].
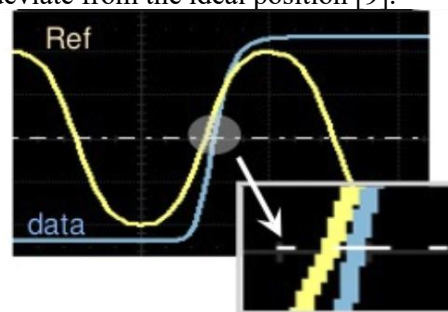

Figure 1. Jitter performance.

There are two types of jitter: deterministic jitter (D_j) and random jitter (R_j). The way these two types of jitter accumulate during serial data communication is different. R_j is considered to be an unbounded component and generally obeys a Gaussian distribution and therefore conforms to certain statistical rules. D_j is considered a bounded component and consists of data-dependent jitter (DD_j), duty-cycle distortion (DCD), periodic jitter (P_j), intersymbol interference (ISI).

D_j is deterministic jitter. It can be predicted and can express specific causes as well. D_j consists of ISI, DCD and P_j, and the amplitude is non-Gaussian and always bounded. D_j depends on the bounded peak to peak.

ISI is inter-symbol interference, which is a data-dependent deterministic jitter that is typically caused by channel scatter or filtering. Inter-code interference, also known as data-dependent jitter

(DD_j), occurs when signals arrive at receiver thresholds at different times, starting at different positions of the bit sequence (symbol).

DCD is the duty cycle distortion. It is the difference between the average pulse width of the positive pulse and the average pulse width of the negative pulse in the clock class code sequence. Amplitude bias error, turn-on delay, and saturation can cause duty cycle distortion.

P_j is periodic jitter, which is repeated in cycles that are independent of data. The typical cause of P_j is the power feedthrough of a switched-mode power supply. The P_j model can be built using one or more sine waves and their harmonics.

R_j is random jitter. R_j R is subject to Gaussian distribution, and theoretically its amplitude is unbounded. The characteristics of the Gaussian distribution depend on the root mean square (RMS) value or standard deviation. It can be easily assumed that, in general, any Gaussian random variable will have a span of 14 times more than the standard deviation in 10^{12} samples. If this span is exceeded in the data communication system, the corresponding bit error rate (BER) is 10^{-12}. R_j is mainly caused by thermal noise in electrical components.
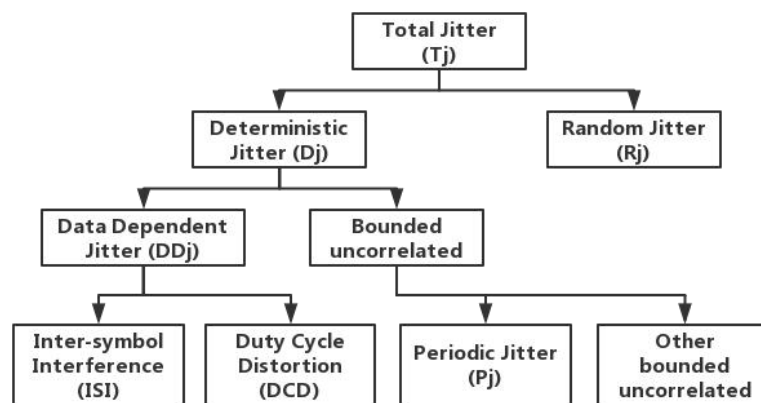
Jitter hierarchy is shown in Figure 2.

Figure 2. Jitter hierarchy.

3. The dual-Dirac model theory

A common method of viewing jitter has traditionally been to look at a sampling scope eye diagram. By setting a window around the crossing point and plotting the number of hits during a measurement. The more samples recorded in a particular position, the more frequently the edges were in that position. This leads to the idea of the histogram being a measure of the probability of an edge falling at a particular location, or time — a Probability Density Function (PDF). The longer the sampling period, the greater the ability to represent rare events such as edges that are further away from the ideal transition timing. When the SDI signal has both deterministic jitter and random jitter, the statistical histogram appears as a bimodal form, shown as Figure3. The probability density function of jitter can be approximated by the Dual-Dirac model.
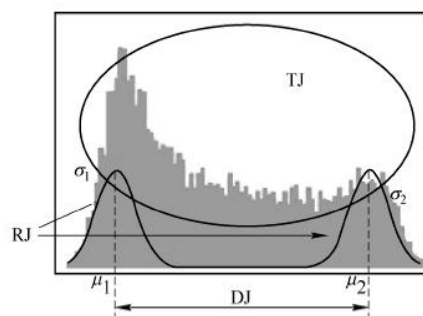

Figure 3. Jitter statistical histogram and dual-Dirac model schematic.

The dual-Dirac model is widely used for its capability in rapid estimating total jitter defined at specified bit error ratio, T_j (BER), and for providing an approach for integrating T_j (BER) from different elements [10]. According to the assumption in [7], total jitter T_j (BER) is the sum of deterministic jitter (D_j) and random jitter (R_j), with R_j weighted by a multiplier α (alpha) that is determined from the bit error ratio[11], represented as (3.1). (α = 14.07 for a typical BER value of 10^{-12}):

$$T_j(BER) = \alpha(BER) * R_j + D_j \tag{3.1}$$

The system corresponds to different coefficient values α in different BER states. The specific numerical correspondence is shown in the following table.

Table 1. Values of $\alpha(BER)$ for different BERs.

BER	$\alpha(BER)$	BER	$\alpha(BER)$
10^{-6}	9.507	10^{-11}	13.412
10^{-7}	10.399	10^{-12}	14.069
10^{-8}	11.224	10^{-13}	14.698
10^{-9}	11.996	10^{-14}	15.301
10^{-10}	12.723	10^{-16}	16.444

R_j and D_j is uncorrelated so the total jitter distribution can be described as the convolution of PDF of R_j and D_j. The jitter distribution can generally be divided into three portions: at the crossing-point, the influence of D_j is dominant; the effect of the intermediate portion R_j is gradually enhanced; and at the asymptotic limit, the shape of the curve is close to R_j distribution. The asymptotic tails of the distribution usually cause errors at the level of BER < 10^{-8}.

The crossing-point is separated into two Dirac-delta functions positioned at μ_1 and μ_2, the D_j dominated region, followed by an artificially abrupt transition to the R_j dominated tails. To implement the dual-Dirac model, we estimated $T_j(BER)$ by describing the tails of the jitter distribution as two Gaussians of width σ separated by a fixed amount $D_j(\delta\delta) \equiv |\mu_1 - \mu_2|$. The model is a Gaussian approximation to the outer edges of the jitter distribution displaced by $D_j(\delta\delta)$. $T_j(BER)$ and its PDF can be represented as (3.2) and (3.3).

$$T_j(BER) = \alpha(BER) * R_j + D_j(\delta\delta) \tag{3.2}$$
$$f_{Tj} = f_{Dj} * f_{Rj} \tag{3.3}$$

In the formula (3.3), f_{Tj}, f_{Dj} and f_{Rj} represent the PDF of T_j, D_j and R_j respectively. It is certainly possible for the components of deterministic jitter to be larger than $D_j(\delta\delta)$, which, as described previously, will be less than D_j (peak-peak).

f_{Rj} is given by a Gaussian distribution whose width is σ and x is the horizontal axis of the eye diagram. Therefore f_{Rj} can be represented as (3.4).

$$f_{Rj}(x) = \frac{1}{\sqrt{2\pi}\sigma} \exp\left(-\frac{x^2}{2\sigma^2}\right) \tag{3.4}$$

Then f_{Tj} can be represented as (3.5).

$$f_{Tj}(x) = \frac{1}{\sqrt{2\pi}\sigma} \int \left[\delta(x' - \mu_1) + \delta(x' - \mu_2)\right] \exp\left(-\frac{(x - x')^2}{2\sigma^2}\right) dx' \tag{3.5}$$

T_j, R_j and D_j are calculated via a fit to the dual-Dirac model, as explained above. P_j, DD_j, ISI and DCD are calculated directly from time interval error measurements. We do not need to fit the middle part of the jitter histogram, because the centre part of the histogram does not contribute to outliers that create bit errors. Which cause bit errors is the tails of jitter histogram. We fit the model to the tails with two parameters: $D_j(\delta\delta)$ and $R_j(\delta\delta)$.

$$R_j(\delta\delta) = \sigma \tag{3.6}$$
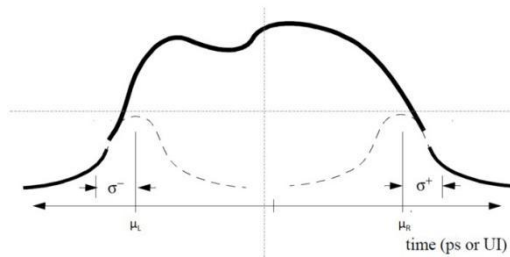$$D_j(\delta\delta) = \mu_2 - \mu_1 \tag{3.7}$$

Figure 4: Illustration of a distribution of TIE jitter values overlaid onto the dual-Dirac jitter model. The outer portions beyond the breaks in the curve represent extrapolated values.

4. Application of the dual-Dirac model

4.1 Time interval error measurement

The algorithms all begin with the acquisition of serial data waveform which include a sufficient number of unit intervals and transitions. Acquiring waveforms should contain more than 10^5 unit intervals and at least 100 iterations of a repeating pattern. It is the way to make the jitter measurements statistical.

First step, we use golden PLL to achieve clock recovery process, which calibrates the expected arrival time of the transition edges of the waveform. The actual arrival time of each edge of the input signal is determined by the method which is cubic interpolation of the samples, shown as Figure 5.
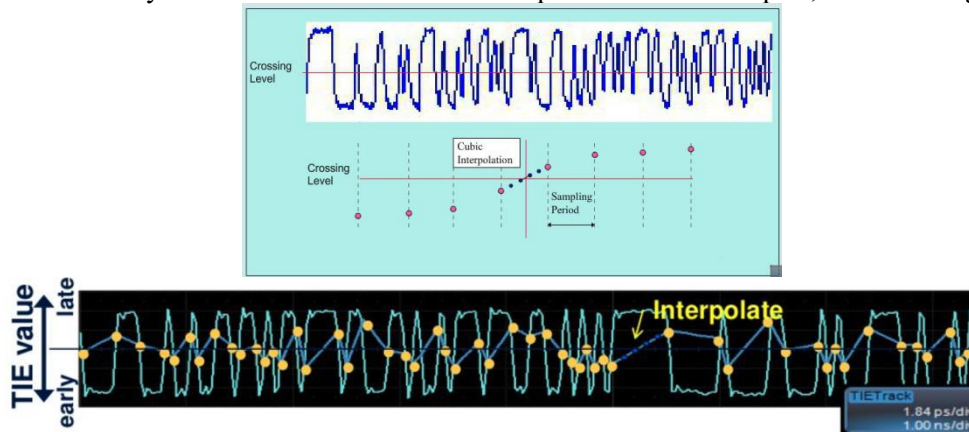

Figure 5. Using interpolation method to identify the arrival time of each edge.

Next, comparing these actual arrival times obtaining from cubic interpolation results to expected arrival times which is represented as the reference clock recovering from the golden PLL outputs. The time interval error (TIE) is obtained by subtracting the actual measured transition time from the expected transition time of the data edge.

4.2 Data-dependent jitter (DD_j) measurement

Pseudo-random sequence of data is commonly used to measure jitter test. In order to locate data-dependent jitter (including *ISI* and *DCD*), we first need to find repeat patterns from the signal. TIE measurements determine an average TIE value for each bit in the repetition pattern. Corresponding

TIE measurements of each iteration of the pattern are averaged resulting in a waveform that contains only data-dependent jitter (DD_j).

The TIE value after a plurality of average calculations is plotted as a histogram. The horizontal axis of the histogram is the moment when the jitter occurs, and the vertical axis is the number of times the jitter occurs, as shown in Figure 6.
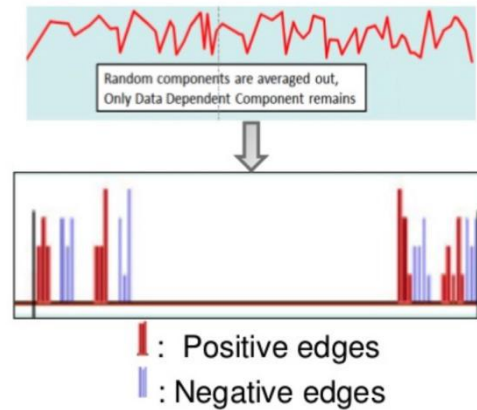

Figure 6. Determine DD_j from TIE.

DD_j, ISI and DCD are determined as follows:

(1) DD_j value is the range of the complete DD_j distribution which is expressed as peak-peak of DD_j histogram, including both positive and negative edges.

(2) ISI value is the larger of the range (max-min) of the individual histograms formed from the DD_j histogram measurements of positive and negative edges.

(3) DCD value is the difference in the means of the histograms for positive and negative edges.

4.3 Pattern Uncorrelated Extraction

To obtain the uncorrelated elements, we shall remove DD_j from TIE. When DD_j is subtracted from full TIE trend, only R_j and bounded uncorrelated jitter whose main component is P_j.

After subtraction, FFT method shall be used to convert waveform to frequency domain. A threshold is set based on the obtained spectral data. Spectral components that exceed the threshold are considered to be caused by periodic jitter. The spectral data information below the threshold is removed leaving only the peak line. Then an inverse FFT is calculated from these isolated P_j peaks. The value for P_j displayed in the jitter measurement table is the peak-to-peak value of the inverse FFT. Figure 8 shows this process.
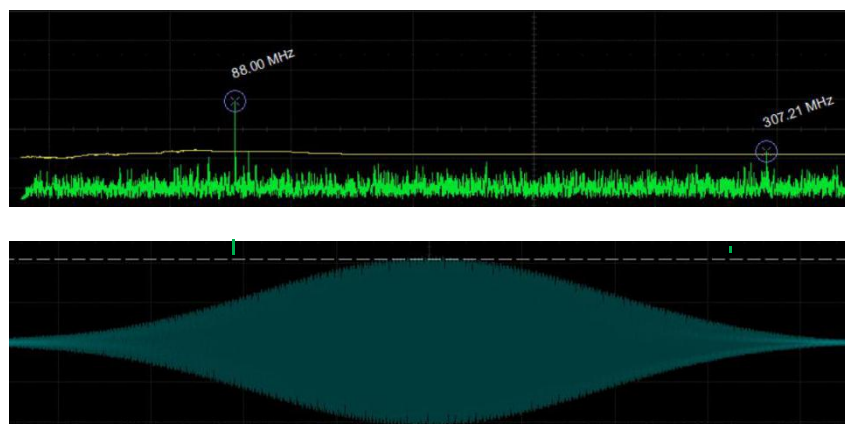

Figure 7. Using FFT to obtain P_j.

4.4 Determine R_j and tail extrapolation

Through the FFT transform we determine P_j and remove it from the spectrum. The remaining spectral components contain random jitter and bounded uncorrelated jitter. In general, the remaining spectral components are integrated and the standard deviation σ value is obtained. The σ value is approximately equal to the value of the random jitter, which is the standard deviation of the Gaussian distribution in the dual-Dirac model, as (3.6) presented.

However, it is important to note that the σ result will also include the effects of bounded, correlated jitter (apart from periodic jitter), including crosstalk. In cases where there is high crosstalk or other bounded uncorrelated jitter, the crosstalk will manifest itself as broadband spectral energy over the frequency range and masquerade as R_j when separated using the spectral method. Therefore, when there is crosstalk or other bounded uncorrelated jitter that raises the jitter spectrum's noise floor, the spectral method can fail to give an accurate result. An adjusted method should be used instead.

In the spectrum method above, the extrapolated tail of total jitter is obeyed by the same Gaussian distribution defaulted, as Figure 4 presented. Here we respectively estimate the extrapolated tails on both sides. Therefore Equation (3.5) will be rewritten as follows:

$$\lim_{x \to -\infty} f_{Tj}(x) \to \frac{1}{\sqrt{2\pi}\sigma_1}\left(-\frac{\left(x-x^{'}\right)^2}{2\sigma_1^2}\right) \tag{4.1}$$

$$\lim_{x \to \infty} f_{Tj}(x) \to \frac{1}{\sqrt{2\pi}\sigma_2}\left(-\frac{\left(x-x^{'}\right)^2}{2\sigma_2^2}\right) \tag{4.2}$$

The next step in the process is the extrapolation of the tails of the jitter distribution. The uncorrelated elements obtained from section 4.3 is used to form a histogram. The tails of this histogram are extrapolated using the σ value found from the spectral analysis.

4.5 Total jitter reconstruction

We convolve the extrapolated histogram with DD_j histogram calculated in section 4.2. The resulting distribution is the overall jitter probability density function (PDF), which looks similar to the TIE Histogram, but with extrapolated tails as described above. The PDF formed is integrated from the outsides to the center to form the cumulative distribution function (CDF). The CDF is plotted with time on the X-axis, and probability on the Y-axis; the width of the CDF at a particular Y-value (or BER) is the T_j at that BER value, as shown in Figure 8.
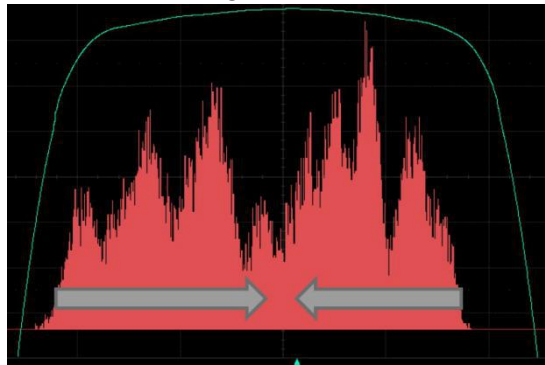

Figure 8. Determine the extrapolated PDF and CDF.

T_j is the width of the CDF at specified BER value. To determine R_j and D_j when using the $R_j + D_j$ CDF Fit method, the CDF is fitted to the Dual Dirac model equation $T_j(BER) = \alpha(BER) * R_j + D_j(\delta\delta)$, where α(BER) is the confidence interval at a confidence level of 1-BER for a single "normal" Gaussian, as shown in (4.3) and (4.4). The points on the CDF that are used in the fit include the selected BER, 1 point above, and two below.

$$T_j(BER) = \alpha(BER) * R_j + D_j(\delta\delta) \qquad (4.3)$$

$$\alpha(BER) = 2\left|CDF^{-1}_{Gaussian}\left(\frac{BER}{2\rho_{tx}}\right)\right| \qquad (4.4)$$

ρ_{tx} is the transition density which means the ratio of the number of logic transitions to the total number of bits.

5. Experiments

In our experiment, we use Tektronix TG700 signal generation platform to output an SDI signal with jitter which can add known deterministic jitter and random jitter to the signal, and use Teledyne LeCroy oscilloscope to measure the signal in time domain. Using 4K SDI video color bar signal as test signal.

In the experiment, test serial data measuring window in oscilloscope should include a sufficient number of unit intervals and transitions. So that the clock recovery process can accurately determine the expected arrival time of the edges, and the jitter calculation, which includes extrapolation, can have the best statistical significance. We use waveforms with a length of more than 100 iterations of a repeating pattern.

We recover the clock signal from SDI using golden PLL software algorithm. The bandwidth of the loop filtering in PLL will directly affect the measurement of the jitter value. If the bandwidth is set too high, the low-frequency periodic component of the jitter in the actual signal may be filtered out and leave only the jitter component caused by the high-frequency phase noise. It will cause errors in the experimental measurement results. In general, the loop filter bandwidth of the PLL in the experimental system needs to be consistent with the filter bandwidth of the PLL circuit in commercial television signal receivers. We set it to 1KHz in measuring process.

Using the signal generation platform to add deterministic jitter and random jitter to the signal and use this signal as the measured signal for jitter analysis experiments. The experimental results are shown in the table below.

Table 2. Jitter measurement data.

	T_j	D_j	R_j
Generator output	1.760ns	360ps	100ps
dual-Dirac spectral R_j direct method	1.913ns	347.5ps	111.3ps
Adjusted dual-Dirac method	1.699ns	358.5ps	95.3ps

The dual-Dirac spectral R_j direct method is used to calculate σ value of the Gaussian distribution and consider the σ value equals to R_j. However, the σ result will also include the effects of bounded, correlated jitter (apart from periodic jitter), and the extrapolated tail of total jitter may not obey the same Gaussian distribution. Therefore the spectral R_j direct method can fail to give an accurate result.

Through the measurement of jitter, on the one hand, it can help us to judge whether the device under test meets the design specifications, and on the other hand, it can help us find the cause of the problem. This is the traceability analysis method of jitter. From the analysis of the cause of jitter and combined with our actual experience and system design, the analysis of the possible increase in jitter lies in the following aspects:

1) interconnection channel;
2) Power supply ripple and noise;
3) Reference clock.

By separating the components of jitter, if the ISI is large, the main source may cause by interconnect channel, and the impedance continuity and loss of the interconnect channel can be further tested to determine the source of the problem. If the P_j is large, it may be caused by power supply ripple (for non-spreading systems). Then further testing of the power supply ripple is necessary to

determine the source of the problem. If the R_j is found to be large, the main reason is heat dissipation and power supply noise.

6. Conclusions

This paper designs a measurement method for high-speed serial digital interface video signal jitter. Jitter measurement and jitter component analysis were performed using an improved dual-Dirac model. The measurement does not depend on BER analysis instrument or other instruments. The measurement and calibration are directly performed by the oscilloscope, which is beneficial to the traceability of the jitter. The experimental results show that the method has better accuracy and the measurement accuracy is higher than the direct spectrum method. The results show that extrapolated tails of total jitter at the asymptotic limit may obey the different Gaussian distribution and the bounded correlation jitter is the part that is easy to be ignored by the measurement, which may have influence on the measurement result.

References

[1]   P. Charles, "Digital Video and HDTV Algorithms and Interfaces," *Morgan Kaufmann Publishers, San Francisco,* vol. 260, p. 630, 2003.

[2]   J. Hudson, "3Gb/s SDI for Transport of 1080p50/60, 3D," *UHDTV1/4k and Beyond,* 2013.

[3]   S. Standard, "2160-Line and 1080-Line Source Image and Ancillary Data Mapping for Single-Link 6G-SDI," 2015.

[4]   S. Standard, "2160-line Source Image and Ancillary Data Mapping for 12G-SDI," 2015.

[5]   M. P. Li, *Jitter, noise, and signal integrity at high-speed*. Pearson Education, 2007.

[6]   R. Stephens, "Analyzing jitter at high data rates," *IEEE Communications Magazine,* vol. 42, no. 2, pp. S6-10 %@ 0163-6804, 2004.

[7]   B. Ham, "Fibre channel-methodologies for jitter and signal quality specification-MJSQ," *Proc. Int. Committee Inf. Technol. Standards (INCITS),* pp. 29-38, 2004.

[8]   H. Chen *et al.*, "Serial digital interface video signal jitter generator and its calibration method," *Measurement,* vol. 106, pp. 116-120 %@ 0263-2241, 2017.

[9]   K. K. Kim, J. Huang, Y.-B. Kim, and F. Lombardi, "Analysis and simulation of jitter sequences for testing serial data channels," *IEEE Transactions on Industrial Informatics,* vol. 4, no. 2, pp. 134-143 %@ 1551-3203, 2008.

[10]   R. Stephens, "Jitter analysis: The dual-Dirac model, RJ/DJ, and Q-scale," *Agilent Technical Note,* 2004.

[11]   R. Stephens, "What the dual-Dirac model is and what it is not," *Tektronix 360 Knowledge Series,* 2006.